Int J Biochem Mol Biol 2024;15(5):127-140
www.ijbmb.org /ISSN:2152-4114/IJBMB0159695

Original Article

Performance prediction of polypeptide derivatives as efficient potential microbial inhibitors: a computational approach

Abel Kolawole Oyebamiji[1,8], Sunday A Akintelu[2,3], Faith Eniola Olujinmi[1], Lukmon Akanni Jinadu[1,6], Oluwakemi Ebenezer[4], Juliana Oluwasayo Aworinde[5], Banjo Semire[7], Jonathan O Babalola[1]

[1]Department of Industrial Chemistry, Bowen University, PMB 284, Iwo, Osun State, Nigeria; [2]Department of Industrial Chemistry, University of Ilesa, Ilesa, Osun State, Nigeria; [3]Good Health and Wellbeing Research Clusters (SDG 03), Department of Industrial Chemistry, University of Ilesa, Ilesa, Osun State, Nigeria; [4]Department of Physics, University of Alberta, Edmonton, AB, Canada; [5]Department of Medical Laboratory Science, Lead City University, Ibadan, Oyo State, Nigeria; [6]Department of Chemical Sciences, Fountain University, Osogbo, Osun State, Nigeria; [7]Department of Pure and Applied Chemistry, Ladoke Akintola University of Technology, Ogbomoso, Oyo State, Nigeria; [8]Good Health and Wellbeing Research Clusters (SDG 03), Bowen University, PMB 284, Iwo, Osun State, Nigeria

Received August 8, 2024; Accepted October 13, 2024; Epub October 15, 2024; Published October 30, 2024

Abstract: Objective: Lately, various scientists have been paying a lot of consideration to the design of operational antimicrobial agents due to the rise of multiple drug-resistant strains. Therefore, this work is aimed at discovering the biochemical behavior of the analyzed polypeptides in relation to glutamine amidotransferase GatD (pdb id: 5n9m) for gram positive bacteria and beta-lactamase class A (pdb id: 5fqq) for gram negative bacteria. Additionally, this study aims to identify the specific atoms involved in the observed biochemical interactions between the studied complexes using computational methods. Methods: In this work, five polypeptides were studied using insilico approach via Spartan 14 software, molecular operating environment, ADMETSar, and Gromacs. Results: The descriptors obtained revealed the activities of the studied compounds, the molecular interaction between the studied ligands as well as glutamine amidotransferase GatD (pdb id: 5n9m) and beta-lactamase class A (pdb id: 5fqq) which thereby exposed compound 1 and 5 to be the compounds with greatest ability to inhibit the studied targets among other studied compounds. Conclusion: Our discoveries may open door for the design of collection of proficient polypeptide-based drug-like compounds as potential anti-microbial agents.

Keywords: Polypeptide, Microbes, MDS, insilico, pharmacokinetics

Introduction

Recently, developments of efficient antimicrobial agents are getting huge consideration from several researchers and this could be due to occurrence of multiple drug resistant [1, 2]. Gram-negative bacterial has been considered to be dangerous bacteria and some gram-positive bacteria has also been observed to be ranked as highest among disease causing agents. *Enterococcus faecium and Staphylococcus aureus* are prominent gram-positive bacteria which displayed resistance to vancomycin and methicillin respectively [3, 4]. More recently, via series of advanced approaches various scientists are now aware of the activities of microbial infections and this has drawn the attention of many researchers to discovering and designing efficient drug-like agents [5, 6]. More so, continuous and overuse of antibiotics has led to resistance of various existing antibiotic agents and this has resulted into development of more efficient drug like agents to combat bacteria globally [6]. Since the discovery of antimicrobial peptides, their mechanisms of action have been the subject of various researches and this has made them to be regarded as special compounds. It's crucial to know the mechanism of action of these antimicrobial peptides in order to advance their development as therapeutic agents. Originally, it was believed that antimicrobial peptides only tar-

https://doi.org/10.62347/YLVH4793

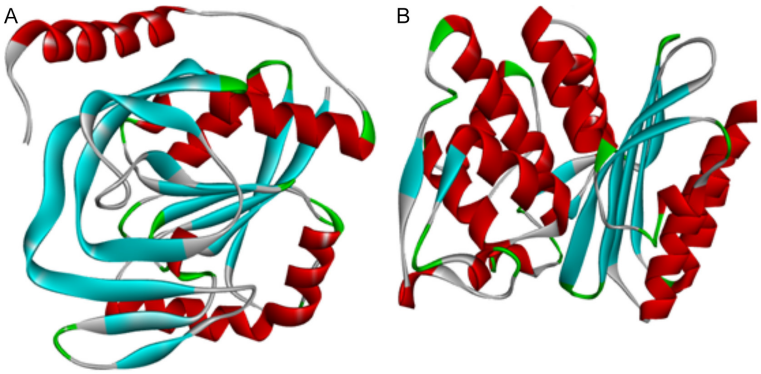

Figure 1. 3-dimensional structure of studied (A) glutamine amidotransferase GatD (B) beta-lactamase class A.

geted the membrane, but there is now growing evidence suggesting that they have additional modes of action. The mode of action (MOA) can be categorized into two main classes: direct killing and immune modulation. Additionally, the direct killing mechanism of action can be further classified into membrane targeting and non-membrane targeting [7-9]. Thus, our laboratory has been involved in the design of efficient polypeptide derivatives in attacking multi-drug-resistant strains.

In medicinal world, both synthetic and natural peptides have drawn the attention of various scientists due to their efficient therapeutic importance [10]. According to Siegel et al., 2020, peptide derivatives with healing capability have been reported to have anti-cancer, anti-fungi and antimicrobial properties [11]. Blanco-Miguez *et al*., 2016 and Wang *et al*., 2022 [12, 13] reported that peptides possess high level of affinity as well as specificity during binding process towards target which thereby activate particular intracellular effects.

Thus, this work is aimed at identifying the biochemical activity of the studied polypeptides towards glutamine amidotransferase GatD (pdb id: 5n9m) [14] for gram positive bacteria and beta-lactamase class A (pdb id: 5fqq) [15] for gram negative bacteria as well as revealing the atoms involved in the biochemical interactions observed between the studied complexes using insilico approach.

Methodology

Induced fit molecular docking

The biochemical activities of eight derivatives of polypeptide were modeled to 2-dimensional format using Chemdraw software [16]. The modeled compounds were subjected to molecular operating environment software (MOE) [17, 18] for optimization via quickprep tool and the optimized compounds were saved in .moe format. Also, glutamine amidotransferase GatD and beta-lactamase class A were retrieved from protein data bank and they were treated and optimized using quickprep tool embedded in molecular operating environment software (**Figure 1**). Also, the binding sites were located and the appropriate site was selected for docking study and the treated receptor were saved in .moe format before docking calculation using induced fit docking method (**Tables 1** and **2**).

Molecular dynamic simulation study

This study was executed via Gromacs software [19] using Charmm force field so as to achieve more understandings into the dynamics of biological complex systems [20]. This study has been observed to give precise results and it has capacity to reveal complicated information about any studied systems that are not easily achievable via experimental approaches; thus, this study was used to investigate the interactions between glutamine amidotransferase GatD (pdb id: 5n9m) for gram positive bacteria and beta-lactamase class A (pdb id: 5fqq) for gram-negative bacteria with compounds 1 and 6. In this work, the studied simulation used TIP3P water for charge maintenance before merging the studied ligands as well as the studied targets. The solvation of the simulated system was achieved in a created container with the introduction of appropriate ions (Na^+ and Cl^-) so as to get the simulated system neutralized [21]. NVT was initiated at 300 K so as to make the simulated system to be stable i.e. to make the volume, temperature and particle features to be steady. In order to maintain the system's pressure and temperature, the system was subjected to another simulation for few minutes. Furthermore, the system was subjected to additional simulation for 100 ns so as to generate the actual binding energy and to

Table 1. Predicted binding site for glutamine amidotransferase GatD

Site	Size	PLB	Hyd	Side	Residues
1	179	4.13	47	97	1:(MET1 HIS2 GLU3 LEU4 THR5 ASN38 THR49 PHE50 ASP51 GLU52 CYS53 ASP54 PRO79 GLU82 ALA83 ASP86 MET88 ARG210 LYS211 ILE213); 2:(ARG128 GLY131 ASP132 GLY145 PHE146 PHE165 PRO191 ILE192 LYS195 ALA228 VAL231 LEU232 ARG235 ALA236 ARG238)
2	131	3.19	34	74	1:(THR5 TYR7 ASP12 LYS13 VAL40 GLU41 ILE42 ASN43 GLU44 THR45 GLU46 GLY47 ILE48 THR49 PHE50 ASP51 GLU52 CYS53); 2:(SER11 ASP12 LYS13 LEU14 ASN15 LEU16 TYR17 ILE20 GLY60 GLY61 SER62 GLU65 ASN148 HIS189 GLY190 PRO191)
3	65	1.82	18	42	1:(LEU16 TYR17 GLY60 GLY61 SER62 ASP63 GLN66 CYS94 GLY95 GLN98 PHE99 TYR104 PRO107 SER124 LYS125 THR126 ARG128 ASN148 HIS149 GLY150 GLY151 TYR187)
4	59	0.97	18	40	2:(THR5 THR49 PHE50 ASP51 GLU52 CYS53 ASP54 PRO79 GLU82 ALA83 ASP86 MET88 PRO89 LYS206 ALA207 ARG210 LYS211)
5	83	0.94	18	42	1:(GLU46 GLY47 THR49); 2:(LEU16 TYR17 GLY60 GLY61 SER62 ASP63 ARG64 GLN66 CYS94 GLY95 GLN98 PHE99 TYR104 PRO107 SER124 LYS125 THR126 ARG128 ASN148 HIS149 GLY150 GLY151 TYR187)
6	28	0.37	5	19	2:(GLU136 SER137 ASP138 THR139 PHE140 GLY158 THR159 LEU160 GLY161 HIS162 LYS175 HIS179)
7	37	0.27	14	31	2:(ARG29 ARG33 THR139 PHE140 TYR197 GLU198 ASP201 TYR202 GLU205 PHE215 LYS218 GLU219 ILE220 ASN222)
8	17	0.16	11	16	2:(MET1 HIS2 ARG33 ASN34 ILE35 ILE213 PRO214 PHE215 GLU216)
9	42	-0.15	11	19	1:(THR5 ARG27 VAL37 ASN38 VAL39 VAL40 GLU41); 2:(ASN15 SER18 GLY21 GLY190 PRO191)
10	25	-0.18	10	18	1:(MET1 HIS2 ARG27 ALA30 LYS31 ASN34 ILE35 LYS36 VAL37)
11	53	-0.21	19	37	1:(MET1 HIS2 GLU3 LYS36 ASN38); 2:(GLY21 ILE24 ALA25 GLN28 PRO191 PRO194 LYS195 ALA224 GLU225 GLN227 ALA228)
12	35	-0.22	16	28	1:(ARG33 THR139 PHE140 TYR197 GLU198 ASP201 TYR202 GLU205 PHE215 LYS218 GLU219)
13	22	-0.23	11	14	1:(VAL163 THR164 PHE165 GLY166 LYS174 LYS241 SER242)
14	6	-0.24	9	14	1:(ILE105 THR106 PRO107 GLU123 SER124 LYS125 ARG152)
15	14	-0.27	11	18	1:(MET1 HIS2 ARG33 ASN34 ILE35 ILE213 PRO214 PHE215 GLU216)
16	24	-0.28	14	26	1:(GLU205 LYS206 CYS208 GLU209 ILE213 PRO214 PHE215 GLU216 LYS218)
17	7	-0.29	8	20	2:(THR153 TYR154 HIS155 ASP156 THR159 ASN169 ASN170 ASP173 LYS175)
18	11	-0.30	11	22	1:(GLY141 THR142 TYR197 GLU198 ILE226 LYS229 GLN230 ILE233)
19	6	-0.30	8	15	1:(THR130 GLY131 ASP132 PHE165 GLN239 LYS240 LYS241 SER242)
20	23	-0.30	7	10	1:(VAL40); 2:(ASN15 LEU16 TYR17 SER18 HIS189 GLY190)
21	19	-0.31	4	14	1:(GLU136 SER137 ASP138 THR139 PHE140 THR159 LEU160 GLY161 HIS162 HIS179)
22	20	-0.33	8	19	1:(THR153 TYR154 HIS155 ASP156 PHE157 THR159 ASN169 ASN170 ASP173 LYS175)
23	12	-0.34	10	13	2:(ARG27 ALA30 LYS31 ILE35 LYS36 VAL37)
24	10	-0.34	12	19	2:(GLU205 CYS208 GLU209 ILE213 PRO214 PHE215 GLU216 LYS218)
25	13	-0.36	11	22	2:(GLY141 THR142 TYR197 GLU198 ILE226 LYS229 GLN230 ILE233)
26	11	-0.41	8	18	2:(ALA25 GLN28 ARG29 PRO194 LYS195 ASN196 TYR197 THR200 GLU225)
27	20	-0.42	8	20	1:(ALA25 GLN28 ARG29 PRO194 LYS195 TYR197 THR200 GLU225)
28	11	-0.45	16	20	1:(ILE58 GLN66 ALA69 THR70 LEU73 GLY95 GLY96 PHE99 LEU100 LEU115)
29	14	-0.45	11	18	2:(MET10 LYS13 ASN43 GLU65 LEU68 ALA69 GLU72)
30	20	-0.45	10	18	1:(HIS2 GLY212 ILE213 PRO214); 2:(VAL231 ASP234 ARG235 ARG238)
31	6	-0.58	2	9	2:(HIS155 ASP156 PHE157 THR159 ASP173 LYS175)
32	6	-0.60	6	13	1:(GLY87 LYS181 ASN182 TYR202 LYS206)
33	7	-0.61	10	13	1:(GLY145 PHE146 ILE192 ALA228 VAL231 LEU232 ARG235)
34	7	-0.61	2	2	1:(THR45 GLU46 GLY47 ILE48 THR49 LYS75 ILE76)
35	7	-0.61	2	2	2:(GLU82 GLU85 ASP86)
36	9	-0.63	8	11	1:(GLN28 LYS31 LYS32)
37	10	-0.68	5	14	1:(GLN28 ARG29 LYS32 ILE220 ASP221 ASN222 GLU225)
38	4	-0.68	4	5	2:(ARG64 ALA67 LEU68)

calculate other parameters such as RMSD, RMSF etc.

Density functional theory method

The 2-dimensional structure of the selected compounds (compound 1 and 6) were modeled using Chemdraw and the structures were subjected to Spartan 14 [22] so as to convert it to 3-dimensional structure prior to optimization using 6-31G** as the basis set. The completion of the optimization resulted to series of calculated descriptors such as highest occupied molecular orbital energy, lowest unoccupied

Table 2. Predicted binding site for beta-lactamase class A

Site	Size	PLB	Hyd	Side	Residues
1	56	2.07	8	37	1:(CYS69 SER70 LYS73 TYR105 SER130 ASN132 GLU166 ASN170 THR216 ARG220 LYS234 THR235 GLY236 THR237 GLY238)
2	32	1.62	17	27	1:(VAL48 LEU49 ASP50 THR53 ARG55 ARG56 PHE57 ALA289 PHE290 HIS292 HIS293 HIS296)
3	35	0.60	15	32	1:(PRO107 VAL108 LYS111 HIS112 MET117 GLU121 GLU124 ALA125 THR128 TYR129)
4	22	0.50	14	19	1:(ILE212 ARG222 LEU225 PRO226 ALA227 TRP229 ARG230 VAL231)
5	19	-0.45	7	16	1:(ARG43 ARG65 PHE66 PRO67 ALA172 ALA173 PRO174 GLY175 ASP176 THR180 THR266 GLU267)
6	16	-0.55	13	21	1:(GLU100 ASP101 VAL103 THR133 ASN136 LEU137 GLU140 TRP165 GLU166)
7	11	-0.56	6	7	1:(GLY224 LEU225 PRO226 ARG284 VAL287 ALA288)
8	13	-0.68	8	12	1:(LYS219 ALA223 ASP273 ASP276 ALA277 ALA280)
9	11	-0.79	5	10	1:(LEU102 VAL103 ASP104 TYR105 SER106 GLU110)
10	20	-0.82	11	17	1:(ALA79 ALA82 ARG83 GLN86 LEU142 ALA147 LEU148 PHE151)
11	11	-0.95	11	14	1:(GLN32 GLU35 LEU36 ARG39 GLU281 LEU285)

Table 3. Binding affinity (kcal/mol) of studied polypeptides (1-8) and one reference drug

	Binding Affinity (kcal/mol)	
	Glutamine amidotransferase GatD (kcal/mol)	Beta-lactamase class A (kcal/mol)
1	-10.0191574	-9.49024963
2	-9.79909039	-9.81384277
3	-9.93531418	-9.43296623
4	-9.45012474	-9.1457777
5	-9.57165146	-9.60503101
6	-9.32006931	-10.0892706
7	-9.33810997	-9.88565922
8	-9.82527733	-9.93792915
Ciprofloxacin	-6.38399506	-5.67510557

molecular orbital energy, energy gap, log p, hydrogen bond donor and hydrogen bond acceptor etc. The names of the studied selected compounds were (4S)-5-(((2S,3S)-1-(((3S,6S,9S,12S,15S,18S,21S)-9-((1H-imidazol-4-yl)methyl)-3-(2-amino-2-oxoethyl)-18-(3-aminopropyl)-12-benzyl-15-((S)-sec-butyl)-6-(4-methylbenzyl)-2,5,8,11,14,17,20-heptaoxo-1,4,7,10,13,16,19-heptaazacyclopentacosan-21-yl)amino)-3-methyl-1-oxopentan-2-yl)amino)-4-((2S)-2-(2-(L-isoleucyl)-4,5-dihydrothiazole-5-carboxamido)-4-methylpentanamido)-5-oxopentanoic acid (1), and (4S)-5-(((2S,3S)-1-(((3S,6S,9S,12S,15S,18S,21S)-9-((1H-imidazol-4-yl)methyl)-3-(2-amino-2-oxoethyl)-18-(3-aminopropyl)-12-benzyl-15-((S)-sec-butyl)-6-(4-methoxybenzyl)-2,5,8,11,14,17,20-heptaoxo-1,4,7,10,13,16,19-heptaazacyclopentacosan-21-yl)amino)-3-methyl-1-oxopentan-2-yl)amino)-4-((2S)-2-(2-(L-isoleucyl)-4,5-dihydrothiazole-5-carboxamido)-4-methylpentanamido)-5-oxopentanoic acid (6).

Analysis of pharmacokinetic properties

The desire to design potential antimicrobial agents has led us to explore the physicochemical features of the selected compounds and the use of online tool has been explored. The selected compounds (1, 6 and reference compound) were loaded in to SwissADMET server (www.swissadme.ch) [23] to convert them to SMILES format and predict physicochemical properties of the ligands. Also, the generated SMILES formats were used in AdmetSAR tool (http://lmmd.ecust.edu.cn/admetsar2/) to appraise the efficiency of the ligands and detect probable toxic effects [24]. The results obtained were in segments which analyzed the absorption, distribution, metabolism, excretion and toxicity aspect of the studied compounds.

Results and discussion

Predicted scoring for the studied complexes

In this study, eight polypeptide-based compounds and ciprofloxacin as referenced compound were docked against glutamine amido-

transferase GatD (pdb id: 5n9m) for gram positive bacteria and beta-lactamase class A (pdb id: 5fqq) for gram-negative bacteria. The results obtained were presented in **Table 3** and the visual representations of the interaction between the studied complexes were displayed in **Tables 4** and **5**.

Predicted root mean square deviation

Figures 2 and **3** showed predicted root mean square deviation for compound 1-5n9m and compound 6-5fqq complexes.

Predicted root mean square fluctuation

This study exposed the suppleness of amino acid residue during binding with atoms in studied compounds through simulation period. This revealed the softness of the studied amino acids in the studied receptors (**Figures 4** and **5**).

Calculated binding energy

The calculated binding energy for compound 1, 6 and ref against Glutamine amidotransferase GatD and beta-lactamase class A were reported in **Tables 6** and **7**.

Analysis of calculated descriptors

The level of reactivity of any molecular compounds could be explained via the obtained calculated descriptors as shown in **Tables 8** and **9**.

Analysis of pharmacokinetic features

The selected compounds (1 and 6) and referenced compound were subjected to pharmacokinetic study (**Table 10**). The factors considered were Blood-Brain Barrier, Human Intestinal Absorption, Caco-2 Permeability, P-glycoprotein Substrate, P-glycoprotein Inhibitor, Renal Organic Cation Transporter for absorption; Subcellular localization for distribution; CYP450 2C9 Substrate, CYP450 2D6 Substrate, CYP-450 3A4 Substrate, CYP450 1A2 Inhibitor, CYP450 2C9 Inhibitor, CYP450 2D6 Inhibitor, CYP450 2C19 Inhibitor, CYP450 3A4 Inhibitor, and CYP Inhibitory Promiscuity for metabolism; and Human Ether-a-go-go-Related Gene Inhi-bition, AMES Toxicity, Carcinogens, Fish Toxicity, Tetrahymena Pyriformis Toxicity, Honey Bee Toxicity, Biodegradation, Acute Oral Toxicity, and Carcinogenicity (Three-class) for toxicity.

Discussion

The steadiness of gram-positive bacteria and their ability to resist antibiotics rely on the complex structure of the cell wall, in which amidated peptidoglycan is crucial and gram-negative bacteria commonly harbor the beta-lactamase, which accounts for about 20% of the plasmid-mediated resistance to ampicillin in this type of bacteria; therefore, inhibition of these enzymes was considered crucial.

As showed in **Table 3**, the calculated scoring revealed the highest binding affinities for every studied compound (1-8) with glutamine amidotransferase GatD and beta-lactamase class A. Remarkably, compound 1 and 6 showed highest binding affinity for glutamine amidotransferase GatD and beta-lactamase class A with -10.0191574 kcal/mol and -10.0892706 kcal/mol respectively. The assessment of all the binding affinities presented for the studied compounds against the two targets showed that the reference compound showed strongest affinity for Glutamine amidotransferase GatD than the studied compounds (1-8) while the calculated binding affinity for compound 6 against beta-lactamase class A also proved to be stronger than the reference compound. The calculated binding obtained in this study were -10.0191574 kcal/mol, -9.79909039 kcal/mol, -9.93531418 kcal/mol, -9.45012474 kcal/mol, -9.57165146 kcal/mol, -9.32006931 kcal/mol, -9.33810997 kcal/mol, and -9.82527733 kcal/mol for studied ligand-Glutamine amidotransferase GatD complex while -9.49024963 kcal/mol, -9.81384277 kcal/mol, -9.43296623 kcal/mol, -9.1457777 kcal/mol, -9.60503101 kcal/mol, -10.0892706 kcal/mol, -9.88565922 kcal/mol, and -9.93792915 kcal/mol for studied ligand-beta-lactamase class A complex. In summary, compound 2-7 showed weaker binding affinity against Glutamine amidotransferase GatD compared to compound 1 and they all have stronger affinity than the reference drug against Glutamine amidotransferase GatD. Also, compound 1-5, 7 and 8 exhibited weaker binding affinity against beta-lactamase class A

Table 4. Ligand-receptor interacting residues of Glutamine amidotransferase GatD and polypeptide-based compound (1-8)

Ligand	Distance	Bond Type	Residue	2D Diagram
1	2.95	H-donor	GLU172	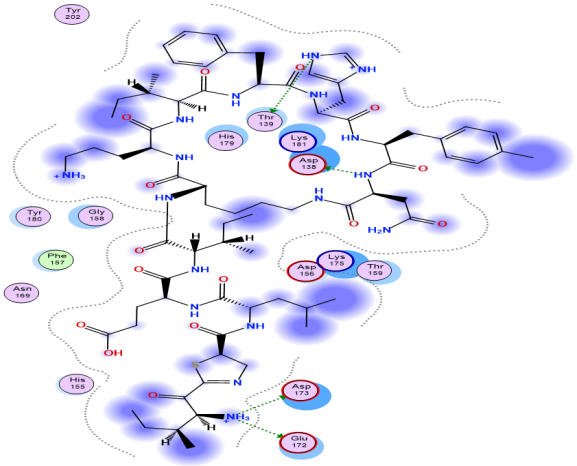
	3.02	H-donor	ASP173	
	3.11	H-donor	THR139	
	2.97	H-donor	ASP138	
	2.95	Ionic	GLU172	
	3.02	Ionic	ASP173	
2	3.04	H-donor	THR130	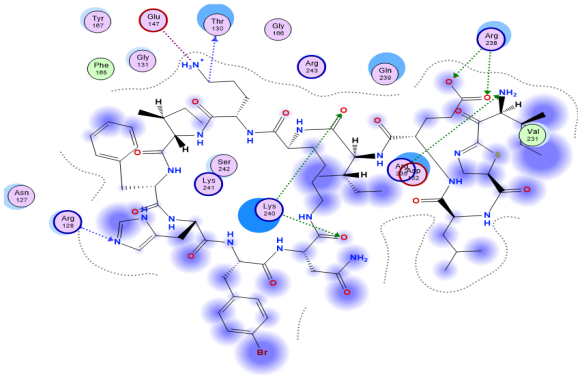
	3.20	H-acceptor	ARG235	
	3.09	H-acceptor	LYS240	
	3.19	H-acceptor	ARG128	
	3.00	H-acceptor	LYS240	
	2.93	H-acceptor	ARG238	
	2.82	H-acceptor	ARG238	
	3.45	Ionic	GLU147	
	2.93	Ionic	ARG238	
	3.67	Ionic	ARG238	
	3.61	Ionic	ARG238	
	2.82	Ionic	ARG238	
3	3.05	H-donor	MET1	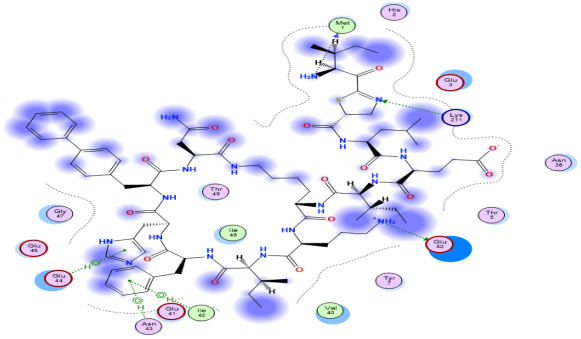
	3.29	H-donor	GLU52	
	3.41	H-acceptor	LYS211	
	3.29	Ionic	GLU52	
	4.59	pi-H	ILE42	
	4.40	pi-H	ASN43	
	3.85	pi-H	GLU44	
4	3.21	H-donor	ASP201	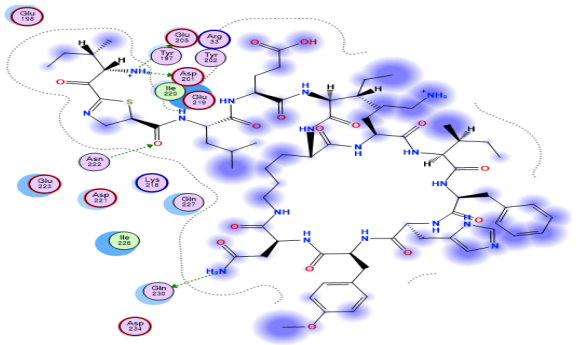
	3.04	H-donor	GLU205	
	3.01	H-donor	GLN230	
	2.90	H-acceptor	ASN222	
	3.21	Ionic	ASP201	
	3.04	Ionic	GLU205	

5	3.30	H-donor	GLU136
	3.00	H-donor	GLU172
	3.03	H-donor	ASP138
	2.50	H-acceptor	THR159
	3.27	H-acceptor	LYS175

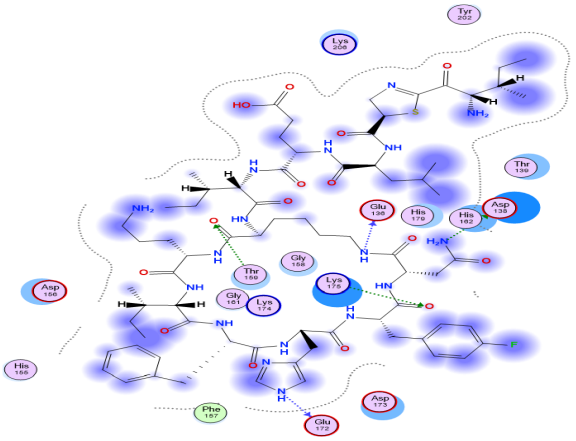

6	3.78	H-donor	ASN15
	3.52	H-donor	LEU16
	2.94	H-acceptor	SER18

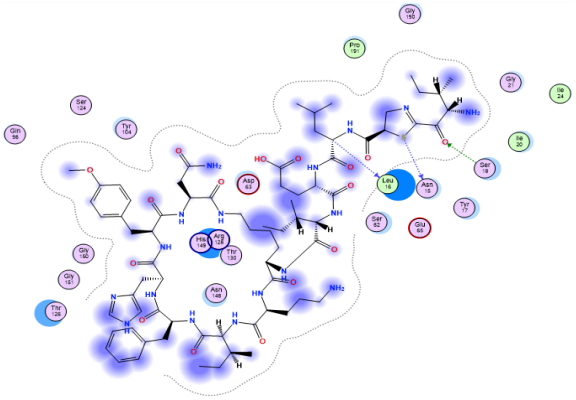

7	3.14	H-donor	ARG128
	3.14	H-donor	ASP171
	3.36	H-acceptor	ARG235
	3.15	H-acceptor	ASN127

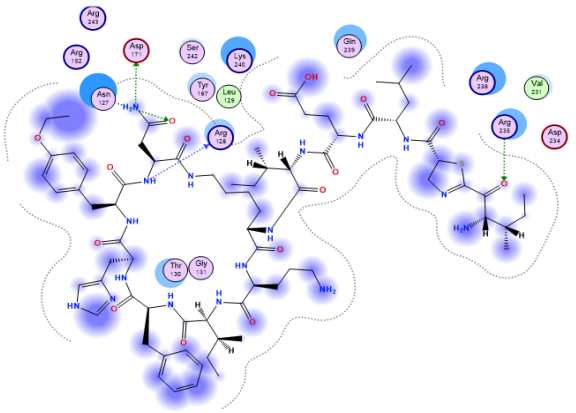

8	3.38	H-donor	SER11

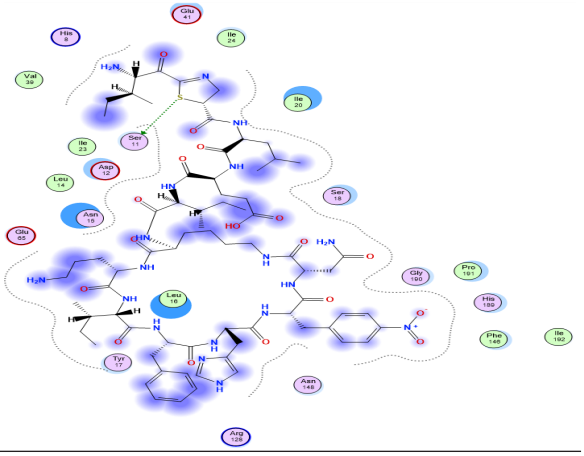

Table 5. Ligand-receptor interacting residues of beta-lactamase class A and polypeptide-based compound (1-8)

Ligand	Distance	Bond Type	Residue	2D Diagram
1	2.65	H-donor	ASP228	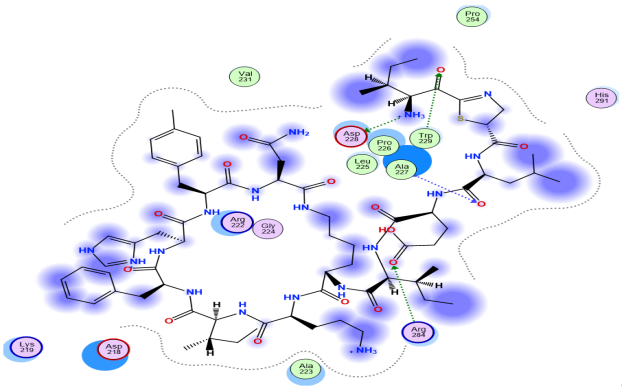
	2.91	H-acceptor	TRP229	
	3.18	H-acceptor	ALA227	
	3.28	H-acceptor	ARG284	
	3.59	Ionic	ASP228	
	2.65	Ionic	ASP228	
2	3.25	H-donor	GLU140	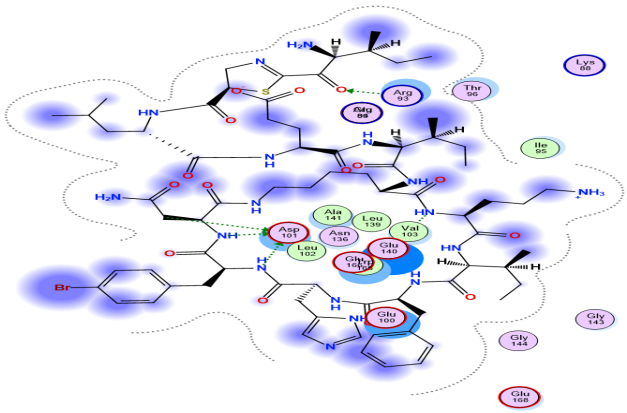
	3.06	H-donor	ASP101	
	3.08	H-donor	ASP101	
	3.34	H-donor	ASP101	
	2.93	H-acceptor	ARG93	
3	3.18	H-donor	LEU195	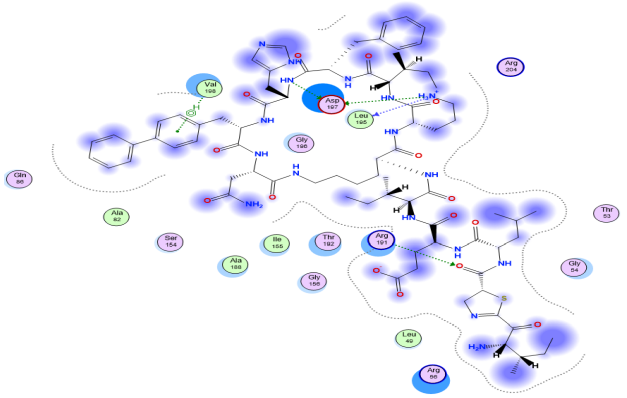
	3.26	H-donor	ASP197	
	3.12	H-donor	ASP197	
	2.76	H-acceptor	ARG191	
	3.26	Ionic	ASP197	
	4.72	pi-H	VAL198	
4	3.05	H-donor	ASN158	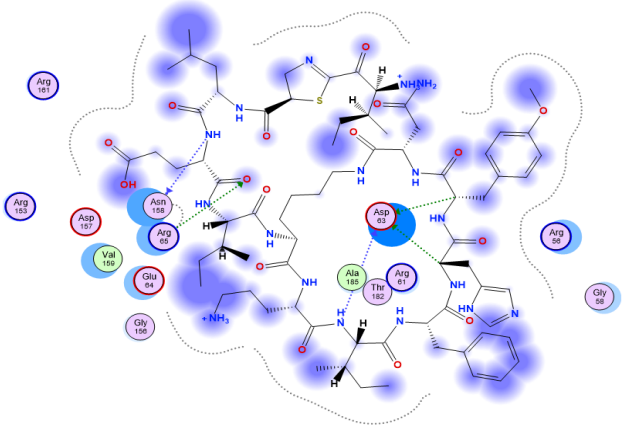
	3.19	H-donor	ASP63	
	3.01	H-donor	ASP63	
	3.50	H-donor	ASP63	
	3.31	H-acceptor	ARG65	

5	2.56	H-donor	ASP228
	3.19	H-acceptor	LYS219
	3.34	H-acceptor	TRP229

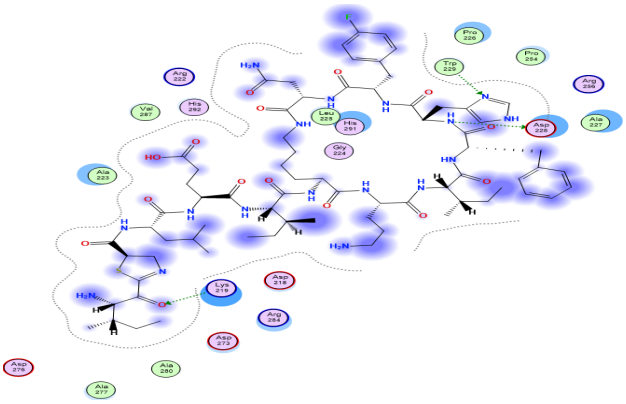

6	3.41	H-acceptor	ARG222
	3.05	H-acceptor	ARG39
	3.45	H-acceptor	ARG284

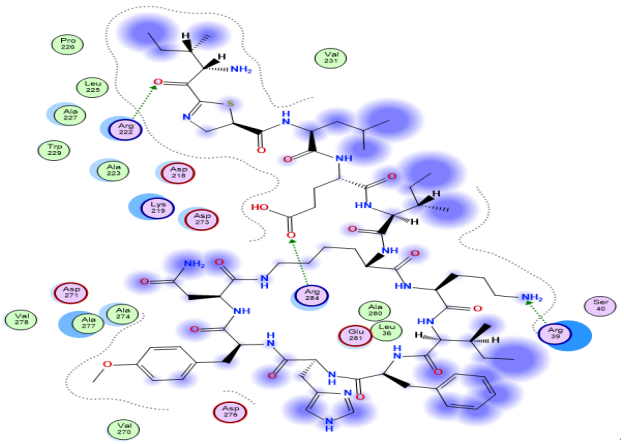

7	3.49	H-donor	VAL198
	3.13	H-donor	SER154
	2.95	H-donor	GLY143
	3.91	pi-H	TRP165

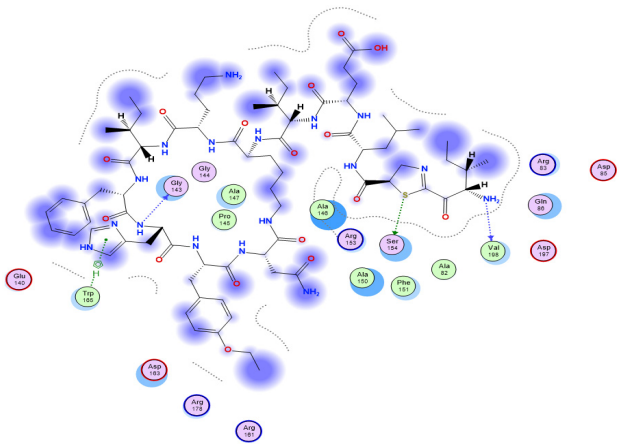

8	2.88	H-donor	ALA223
	2.84	H-acceptor	ARG284
	3.07	H-acceptor	LYS219

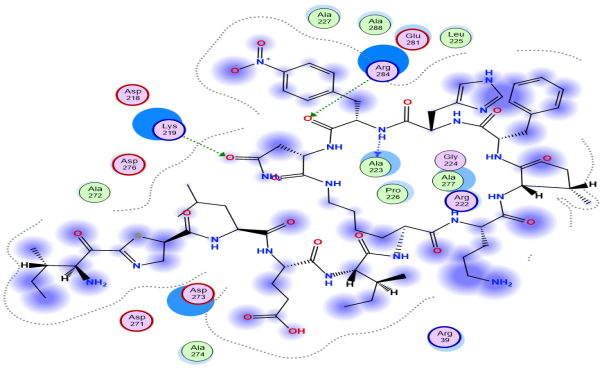

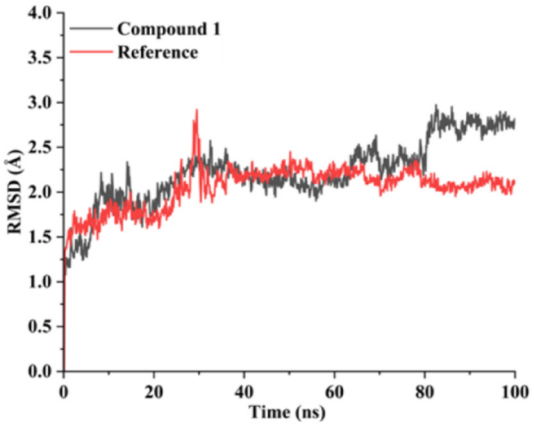

Figure 2. Predicted RMSD of compound 1-5n9m (black) and reference compound-5n9m (red) complexes.

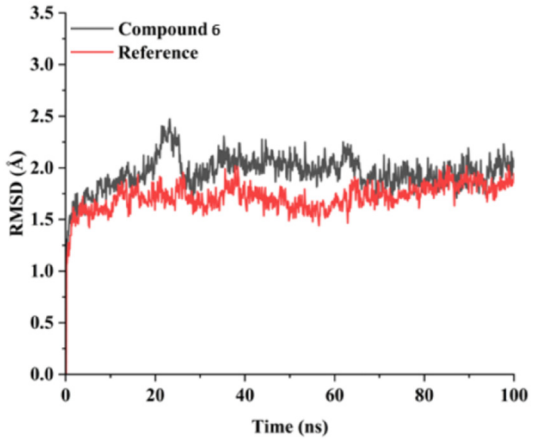

Figure 3. Predicted RMSD of compound 6-5fqq (black) and reference compound-5fqq (red) complexes.

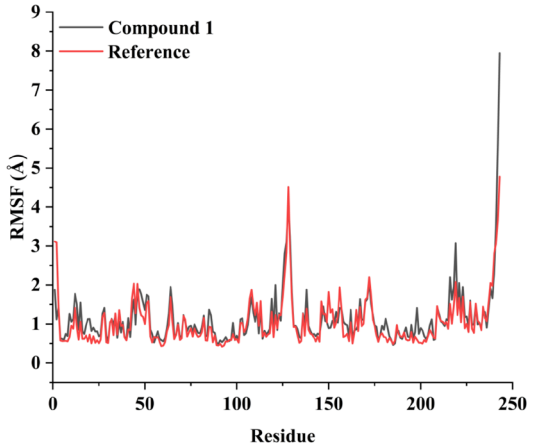

Figure 4. Predicted RMSF of compound 1-5n9m (black) and reference compound-5n9m (red) complexes.

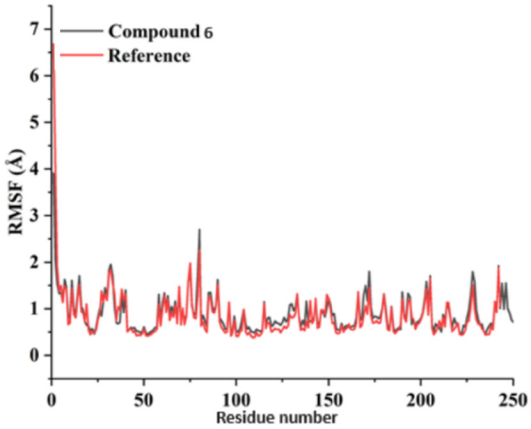

Figure 5. Predicted RMSF of compound 6-5fqq (black) and reference compound-5fqq (red) complexes.

Table 6. Calculated free energies for compound 1-5n9m and ref-5n9m

	ΔG_{gas}	ΔG_{solv}	ΔG_{bind}
Compound 1	-645.2468	624.2081	-21.0386
Reference	-290.7530	258.3767	-32.3763

Table 7. Calculated free energies for compound 6-5fqq and ref-5fqq

	DELTA G_{gas}	DELTA G_{solv}	MMGBSA
Compound 6	-325.4859	287.8545	-37.6314
Reference	-208.1475	191.7084	-16.4391

Table 8. Calculated descriptors for the studied compounds

	HOMO (eV)	LUMO (eV)	Energy Gap (eV)
1	-3.52	-2.35	1.17
6	-3.38	-2.26	1.12

compared to compound 6; however, they all exhibited stronger affinity than the reference compound against beta-lactamase class A.

More so, the inhibiting activity of the studied compounds could be attributed to differences in their chemical structures and the visual representations of the docked complexes against the studied targets were presented in **Tables 4** and **5**. Therefore, the induced fit method used in this work suggests that compound 1 and 6 hold promising potential as gram-positive and gram-negative inhibitors respectively.

Table 9. Predicted HOMO-LUMO overlay

	HOMO	LUMO
1	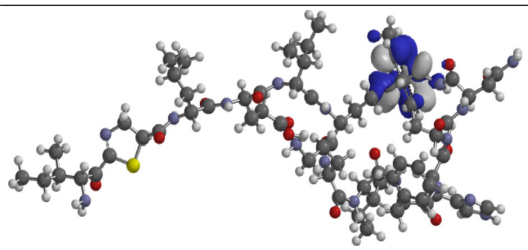	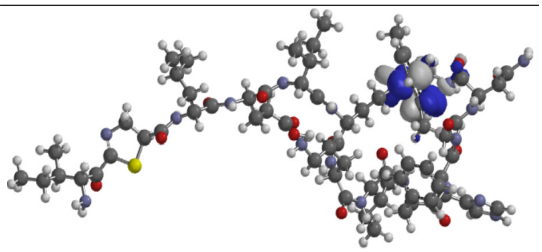
6	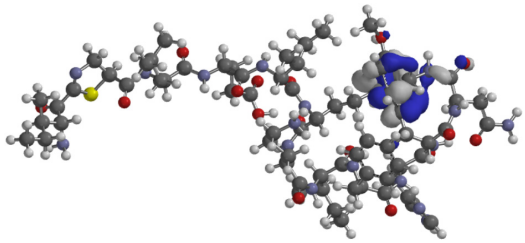	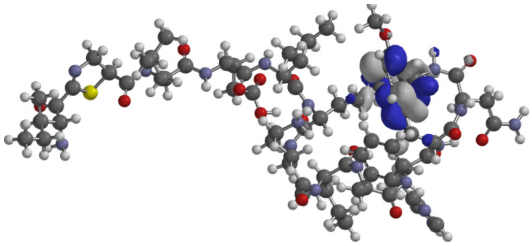

Figures 2 and **3** exposed the backbone atoms which were linked to the original configuration of the receptors under study in developing complexes with compounds 1, 6 as we as the referenced compound during the 100 ns MD simulation. This work was executed so as to examine the extent of nonconformity from the preliminary configuration after binding as well as the stability of the simulated complexes. In this work, the structure of compound 1-5n9m was observed to be fairly stable when compared to the structure of the referenced compound-5n9m complex. Also, the configuration of compound 6-5fqq was stable than the structure predicted for the reference-5fqq complex.

Figure 4 showed a fair resemblance in the pattern at which the studied amino acid fluctuates while the resemblance observed in **Figure 5** in the pattern at which the studied amino acid fluctuates was better. Also, the disparity detected between the compound 6-5fqq was not as much as compound 1-5n9m and this showed that the pattern revealed in **Figure 5** explained that compound 6-5fqq demonstrated a slight degree of nonconformity which signifies that compound 6 has greater level of affinity towards 5fqq.

In this work, the energy calculated was ΔG_{gas}, ΔG_{solv} and ΔG_{bind}. As shown in **Table 6**, it was observed that compound 1 showed a weak tendency to inhibit Glutamine amidotransferase GatD compared to the rate at which the reference compound revealed the ability to inhibit Glutamine amidotransferase GatD while compound 6 has better tendency to inhibit beta-lactamase class A than the reference compound. The calculated binding energy were -645.2468 kcal/mol (ΔG_{gas}), 624.2081 kcal/mol (ΔG_{solv}) and -21.0386 kcal/mol (ΔG_{bind}) for compound 1-5n9m and -290.7530 kcal/mol (ΔG_{gas}), 258.3767 kcal/mol (ΔG_{solv}) and -32.3763 kcal/mol (ΔG_{bind}) for ref-5n9m. Also, the calculated binding energy for compound 6-5fqq was -325.4859 kcal/mol, 287.8545 kcal/mol, -37.6314 kcal/mol and -208.1475 kcal/mol, 191.7084 kcal/mol, -16.4391 kcal/mol are for ref-5fqq.

In addition, compounds with highest donating and receiving power of electrons are expected to display high potential of reacting strongly with the neighboring compounds; thus, compound 6 and 1 exhibited the highest power to react strongly compared to other studied compounds. The order of calculated HOMO energy value is 6 > 1 and the order of calculated LUMO energy is 1 > 6 (**Figures 6** and **7**). Also, the report showed in **Table 8** revealed that compound 1 and 6 has high level of reactivity. It was reported that enhanced level of reactivity of any compound could also be attributed to the lower energy gap, thus, the derivative attached to the parent compound was observed to be responsible for lower energy gap which thereby is expected to enhance its reactivity. The calculated HOMO, LUMO and energy gap

Table 10A. ADMET predicted profile --- classification

Model	Compound 1		Compound 6		Reference compound	
	Result	Probability	Result	Probability	Result	Probability
Absorption						
Blood-Brain Barrier	BBB-	0.9965	BBB-	0.9969	BBB-	0.9655
Human Intestinal Absorption	HIA-	0.6906	HIA-	0.8546	HIA+	0.9795
Caco-2 Permeability	Caco2-	0.7747	Caco2-	0.7642	Caco2-	0.8956
P-glycoprotein Substrate	Substrate	0.7903	Substrate	0.8255	Substrate	0.7862
P-glycoprotein Inhibitor	Non-inhibitor	0.7823	Non-inhibitor	0.8135	Non-inhibitor	0.8852
	Non-inhibitor	0.8285	Non-inhibitor	0.8323	Non-inhibitor	0.8981
Renal Organic Cation Transporter	Non-inhibitor	0.8471	Non-inhibitor	0.8179	Non-inhibitor	0.7288
Distribution						
Subcellular localization	Mitochondria	0.4534	Mitochondria	0.4704	Lysosome	0.4667
Metabolism						
CYP450 2C9 Substrate	Non-substrate	0.7194	Non-substrate	0.7194	Non-substrate	0.8481
CYP450 2D6 Substrate	Non-substrate	0.7732	Non-substrate	0.7732	Non-substrate	0.9116
CYP450 3A4 Substrate	Substrate	0.5367	Substrate	0.5367	Non-substrate	0.7633
CYP450 1A2 Inhibitor	Non-inhibitor	0.9080	Non-inhibitor	0.9080	Non-inhibitor	0.7735
CYP450 2C9 Inhibitor	Non-inhibitor	0.8437	Non-inhibitor	0.8437	Non-inhibitor	0.9070
CYP450 2D6 Inhibitor	Non-inhibitor	0.8990	Non-inhibitor	0.8990	Non-inhibitor	0.9231
CYP450 2C19 Inhibitor	Non-inhibitor	0.8211	Non-inhibitor	0.8211	Non-inhibitor	0.9025
CYP450 3A4 Inhibitor	Non-inhibitor	0.7173	Non-inhibitor	0.7173	Non-inhibitor	0.8309
CYP Inhibitory Promiscuity	Low CYP Inhibitory Promiscuity	0.7755	Low CYP Inhibitory Promiscuity	0.7755	Low CYP Inhibitory Promiscuity	0.6150
Human Ether-a-go-go-Related Gene Inhibition	Weak inhibitor	0.9919	Weak inhibitor	0.9877	Weak inhibitor	0.8366
	Inhibitor	0.6066	Inhibitor	0.7399	Non-inhibitor	0.6855
AMES Toxicity	Non AMES toxic	0.7019	Non AMES toxic	0.6685	AMES toxic	0.8851
Carcinogens	Non-carcinogens	0.8836	Non-carcinogens	0.8957	Non-carcinogens	0.8431
Fish Toxicity	High FHMT	0.9788	High FHMT	0.9876	High FHMT	0.9937
Tetrahymena Pyriformis Toxicity	High TPT	0.9759	High TPT	0.9783	High TPT	0.8218
Honey Bee Toxicity	Low HBT	0.7735	Low HBT	0.7262	Low HBT	0.8889
Biodegradation	Not ready biodegradable	0.9846	Not ready biodegradable	0.9866	Not ready biodegradable	1.0000
Acute Oral Toxicity	III	0.5733	III	0.5658	III	0.7731
Carcinogenicity (Three-class)	Non-required	0.5858	Non-required	0.5883	Non-required	0.6119

Table 10B. ADMET predicted profile --- regression

Model	Value	Unit	Value	Unit	Value	Unit
Absorption						
Aqueous solubility	-3.3465	LogS	-3.3985	LogS	-3.4638	LogS
Caco-2 Permeability	-0.2896	LogPapp, cm/s	-0.3107	LogPapp, cm/s	0.8090	LogPapp, cm/s
Toxicity						
Rat Acute Toxicity	2.8866	LD50, mol/kg	2.8763	LD50, mol/kg	2.1882	LD50, mol/kg
Fish Toxicity	1.5476	pLC50, mg/L	1.4360	pLC50, mg/L	1.3310	pLC50, mg/L
Tetrahymena Pyriformis Toxicity	0.4463	plGC50, ug/L	0.5148	plGC50, ug/L	0.5304	plGC50, ug/L

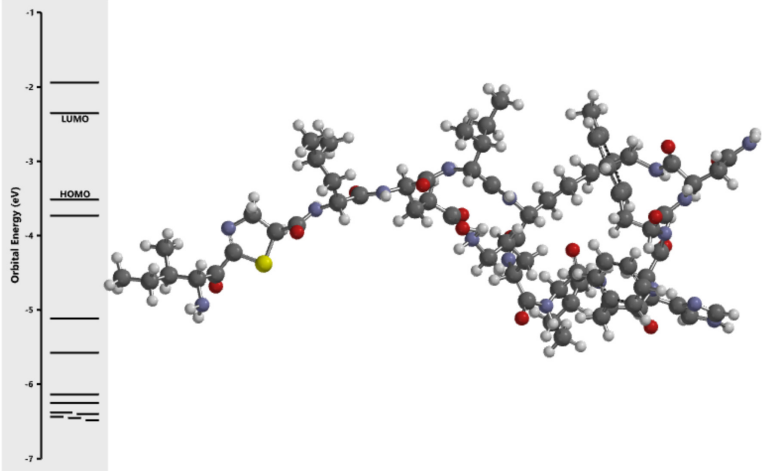

Figure 6. Orbital energy profile for compound 1.

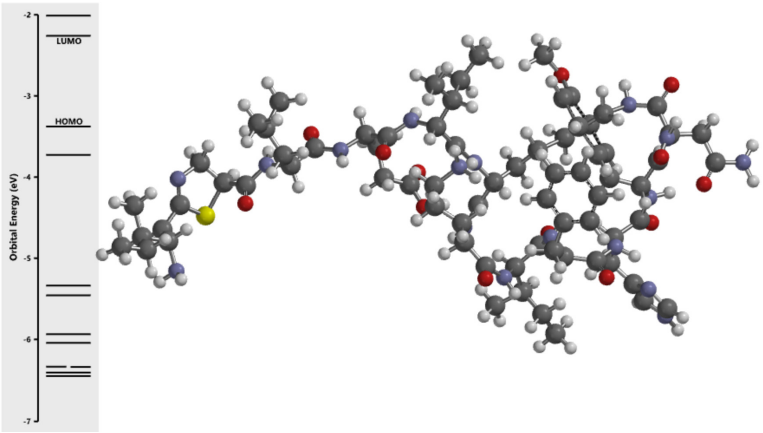

Figure 7. Orbital energy profile for compound 6.

were -3.52 eV, -2.35 eV and 1.17 for compound 1; -3.42 eV, -2.40 eV, 1.02 eV for compound 5 and -4.08 eV, -2.82 eV and 1.26 eV for reference compound (**Table 9**).

The value obtained for the selected compounds were within the same range with the reference compound and this signifies that the selected studied compounds have ability to act as drug and it showed that it is fair for oral absorption (**Table 10**).

Conclusion

Investigating the bioactivities of the polypeptides and assessing the inhibiting potential of these compounds against glutamine amidotransferase GatD (pdb id: 5n9m) and beta-lactamase class A (pdb id: 5fqq) was the focus of this study. The calculated binding affinity of the individual complexes revealed that compound 1 and 6 demonstrated the highest potential for inhibiting both glutamine amidotransferase GatD and beta-lactamase class A compared to the other compounds studied. Molecular dynamic simulation studies confirmed the inhibiting activities of the selected compounds. The optimization of compounds 1 and 6 resulted in various descriptors, shedding light on their nature and reactivity levels.Furthermore, notable correspondences were observed between the pharmacokinetic properties of compounds 1 and 6 and reference compound.

Disclosure of conflict of interest

None.

Address correspondence to: Abel Kolawole Oyebamiji, Department of Industrial Chemistry, Bowen University, PMB 284, Iwo, Osun State, Nigeria. E-mail: abeloyebamiji@gmail.com; akintelusundayadewale@gmail.com

References

[1] Padiyara P, Inoue H and Sprenger M. Global governance mechanisms to address antimicrobial resistance. Infect Dis (Auckl) 2018; 11: 1178633718767887.

[2] Patil SA, Nesaragi AR, Rodríguez-Berrios RR, Hampton SM, Bugarin A and Patil SA. Coumarin triazoles as potential antimicrobial agents. Antibiotics (Basel) 2023; 12: 160.

[3] Strzelecka M and Swiątek P. 1,2,4-triazoles as important antibacterial agents. Pharmaceuticals (Basel) 2021; 14: 224.

[4] Duval RE, Grare M and Demoré B. Fight against antimicrobial resistance: we always need new antibacterials but for right bacteria. Molecules 2019; 24: 3152.

[5] El Malah T, Nour HF, Satti AAE, Hemdan BA and El-Sayed WA. Design, synthesis, and antimicrobial activities of 1,2,3-triazole glycoside clickamers. Molecules 2020; 25: 790.

[6] von Wintersdorff CJ, Penders J, van Niekerk JM, Mills ND, Majumder S, van Alphen LB, Savelkoul PH and Wolffs PF. Dissemination of antimicrobial resistance in microbial ecosystems through horizontal gene transfer. Front Microbiol 2016; 7: 173.

[7] Kumar P, Kizhakkedathu JN and Straus SK. Antimicrobial peptides: diversity, mechanism of action and strategies to improve the activity and biocompatibility in vivo. Biomolecules 2018; 8: 4.

[8] Zhang L, Rozek A and Hancock RE. Interaction of cationic antimicrobial peptides with model membranes. J Biol Chem 2001; 276: 35714-35722.

[9] Ulm H, Wilmes M, Shai Y and Sahl HG. Antimicrobial host defensins - specific antibiotic activities and innate defense modulation. Front Immunol 2012; 3: 249.

[10] Nhàn NTT, Yamada T and Yamada KH. Peptide-based agents for cancer treatment: current applications and future directions. Int J Mol Sci 2023; 24: 12931.

[11] Siegel RL, Miller KD and Jemal A. Cancer statistics, 2020. CA Cancer J Clin 2020; 70: 7-30.

[12] Blanco-Miguez A, Gutiérrez-Jácome A, Pérez-Pérez M, Pérez-Rodríguez G, Catalán-García S, Fdez-Riverola F, Lourenço A and Sánchez B. From amino acid sequence to bioactivity: the biomedical potential of antitumor peptides. Protein Sci 2016; 25: 1084-1095.

[13] Wang L, Wang N, Zhang W, Cheng X, Yan Z, Shao G, Wang X, Wang R and Fu C. Therapeutic peptides: current applications and future directions. Signal Transduct Target Ther 2022; 7: 48.

[14] Leisico F, V Vieira D, Figueiredo TA, Silva M, Cabrita EJ, Sobral RG, Ludovice AM, Trincao J, Romao MJ, de Lencastre H and Santos-Silva T. First insights of peptidoglycan amidation in Gram-positive bacteria - the high-resolution crystal structure of Staphylococcus aureus glutamine amidotransferase GatD. Sci Rep 2018; 8: 5313.

[15] Risso VA, Martinez-Rodriguez S, Candel AM, Kruger DM, Pantoja-Uceda D, Ortega-Munoz M, Santoyo-Gonzalez F, Gaucher EA, Kamerlin SCL, Bruix M, Gavira JA and Sanchez-Ruiz JM. De novo active sites for resurrected Precambrian enzymes. Nat Commun 2017; 8: 16113.

[16] Oyebamiji AK, Akintelu SA, Akintayo ET, Akintayo CO, Ebenezer O, Ogunlakin AD, Ojo OA and Babalola JO. Integrated approach for studying anti-angiotensin converting enzyme activity of triazole derivatives to down-regulate diabetes. J Phytomed Therapeutics 2024; 23: 1293.

[17] Omotayo IA, Banjo S, Emmanuel OT, Felix LD, Kolawole OA, Dele OA, Olasegun AI, Dasola AM and Ayobami OO. Molecular properties and In silico bioactivity evaluation of (4-fluorophenyl) [5)-3-phen-(4-nitrophenyl yl-4,5-dihydro-1 H-pyrazol-1-yl]methanone derivatives: DFT and molecular docking approaches. J Taibah Univ Med Sci 2023; 18: 1386-1405.

[18] Oke AM, Adelakun AO, Akintelu SA, Soetan EA, Oyebamiji AK and Ewemoje TA. Inhibition of angiotensin converting enzyme by phytochemicals in Cucurbita pepo L.: in silico approach. Pharmacological Research - Modern Chinese Medicine 2022; 4: 100142.

[19] Van Der Spoel D, Lindahl E, Hess B, Groenhof G, Mark AE and Berendsen HJ. GROMACS: fast, flexible, and free. J Comput Chem 2005; 26: 1701-1718.

[20] Showalter SA and Brüschweiler R. Validation of molecular dynamics simulations of biomolecules using NMR spin relaxation as benchmarks: application to the AMBER99SB force field. J Chem Theory Comput 2007; 3: 961-975.

[21] Hansson T, Oostenbrink C and van Gunsteren W. Molecular dynamics simulations. Curr Opin Struct Biol 2002; 12: 190-196.

[22] Semire B, Abdulsalami IO, Latona DF, Oyebamiji AK, Owonikoko AD, Obiyenwa KG and Odunola OA. Effect of seleno-thiophene π-linkers on electronic and photovoltaic properties of boro-phenothiazine donors for DSSCs application: TD-DFT and DFT methods. Russ J Phys Chem A 2024; 98: 156-168.

[23] Daina A, Michielin O and Zoete V. SwissADME: a free web tool to evaluate pharmacokinetics, drug-likeness and medicinal chemistry friendliness of small molecules. Sci Rep 2017; 7: 42717.

[24] Kim S, Chen J, Cheng T, Gindulyte A, He J, He S, Li Q, Shoemaker BA, Thiessen PA, Yu B, Zaslavsky L, Zhang J and Bolton EE. PubChem in 2021: new data content and improved web interfaces. Nucleic Acids Res 2021; 49: D1388-D1395.